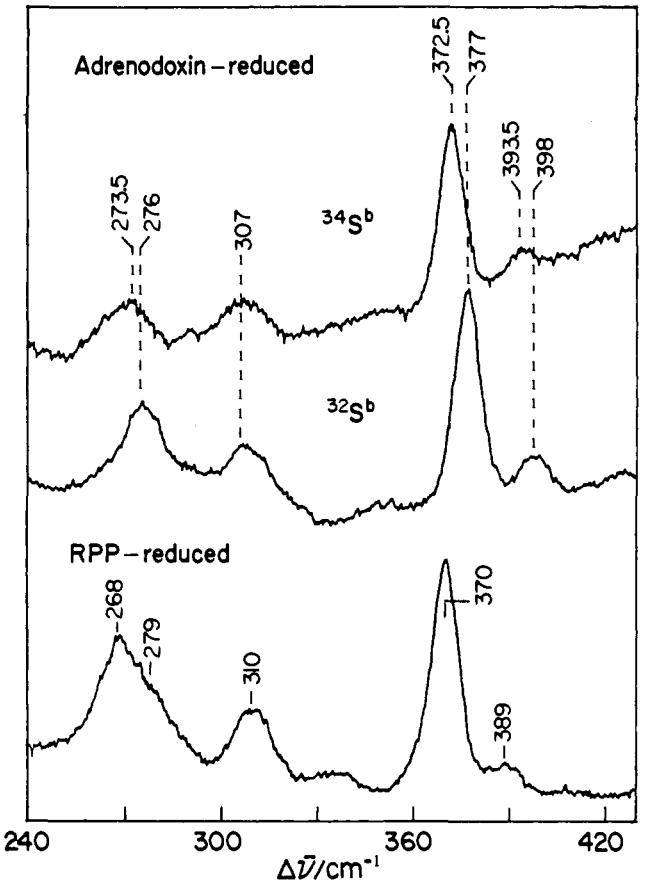

Figure 9. Resonance Raman spectra (77 K) of reduced Ado and *C. pastuerianum* RPP obtained with 530.9- and 568.2-nm excitations, respectively, and 6-cm^{-1} slit widths (0.5-cm^{-1} increments).

of H bonds to the cysteine S atoms). As seen in Table V, good results were obtained with a $K(Fe^{II}-S)/K(Fe^{III}-S)$ force constant ratio of 0.7. The high-frequency bridging modes, $B_{2u}{}^b$ (421 cm^{-1}) and $A_g{}^b$ (393 cm^{-1}) shift down by the observed intervals, and the remaining bands are calculated to group together so that their overlapping contributions could easily account for the broad 307- and 276-cm^{-1} features. Since the electronic transition providing the resonance enhancement is undoubtedly a $S \rightarrow Fe^{III}$ CT transition, it is reasonable to assume that most of the RR intensity is associated with coordinates centered on the Fe^{III} side of the complex. Indeed, the calculated potential energy distribution (Table V) does give a rough guide to the RR intensities, and it is not surprising that the 377-cm^{-1} band is the strongest one in the reduced spectrum, since it involves bonds to the Fe^{III} almost exclusively. On the other hand, the strong 291-cm^{-1} band in the oxidized Ado spectrum, $B_{3u}{}^t$, correlates with a band which is mainly Fe^{II}–S stretching in character, calculated to fall at 258 cm^{-1} in the reduced spectrum. Failure to observe this band can be attributed to its Fe^{II}–S character.

Conclusions

RR spectra have been assigned for the major classes of Fe_2S_2 proteins. All of the Fe–S stretching bands are activated, including the infrared bands which are inactive in analogue RR spectra. This activation implies an asymmetric protein environment, suggested to be due to differential H-bonding to the cysteine S atoms on the two ends of the complex. Strong activation of the ~290-cm^{-1} $B_{3u}{}^t$ mode is attributable to its out-of-phase breathing character. The frequencies of corresponding bands vary appreciably among the three proteins and the analogue complexes. This variation is attributed to increased bridging and terminal Fe–S bond strengths in the protein relative to the analogues, due to protein compression effects or to stabilizing H-bond interactions which ameliorate the negative charge on the complex. In addition there is evidence in Fd for Fe–S–C–C dihedral angles somewhat greater than 90°, allowing mixing of the S–C–C bending coordinates with the terminal Fe–S stretches. Pronounced differences are also seen in the RR enhancement patterns, indicating that the resonant $S \rightarrow Fe$ CT transitions are altered by the structural variations. RR spectra of reduced Ado and RPP are in accord with a localized model in which the Fe–S bond strength is reduced by ~30% upon reduction and enhancement is provided by the CT transitions to the unreduced Fe.

Acknowledgment. This work was supported by NIH Grant GM13498 (to T.G.S.).

Novel Cytotoxic and Phytotoxic Halogenated Sesquiterpenes from the Green Alga *Neomeris annulata*[1]

David E. Barnekow,[†] John H. Cardellina, II,*[,†] Andrew S. Zektzer,[‡,2] and Gary E. Martin[‡]

Contribution from the Natural Products Laboratory, Department of Chemistry, Montana State University, Bozeman, Montana 59717, and Department of Medicinal Chemistry, College of Pharmacy, University of Houston, Houston, Texas 77004. *Received June 13, 1988*

Abstract: The cytotoxicity and phytotoxicity observed in extracts of the calcareous green alga *Neomeris annulata* were traced to a fraction containing a trio of new halogenated sesquiterpenes. The application of zero-quantum and reverse-detected multiple-quantum 2D NMR techniques was pivotal in the elucidation of the structures. Three different, seemingly biosynthetically related carbon skeletons, one of them (neomeranol) unprecedented, are represented by these constitutional isomers. While a few halogenated phenols and quinones are known from green algae, this is the initial discovery of halogenated sesquiterpenes in the Chlorophyta.

Neomeris annulata is a diminutive calcareous green alga widely distributed in the shallow, inshore waters of Bermuda. The organic soluble extracts of collections made in 1984 and 1986 exhibited phytotoxicity to johnsongrass, brine shrimp toxicity, and marginal cytotoxicity (KB: ED_{50} 29 μg/mL) in our pharmacological/agrochemical screening program. Bioassay guided fractionation traced the activities observed to a trio of new monobrominated sesquiterpene alcohols. This is the first report of halogenated sesquiterpenes from a green alga and the first association of

[†] Montana State University.
[‡] University of Houston.

(1) Contribution No. 1123 from the Bermuda Biological Station and from the Montana Agricultural Experiment Station.
(2) Current address: Abbott Laboratories, N. Chicago, IL.

0002-7863/89/1511-3511$01.50/0

Table I. NMR Data of *Neomeris* Sesquiterpenes (**1**, **4**, **5**)[a,b]

carbon no.	1		4		5	
1	67.5 (d)	3.55 (dd, J = 13.0, 3.8)	47.8 (t)	2.25 (t, J = 13.0); 1.80 (m, J = 13.0, 4.4)	59.0 (d)	4.35 (t, J = 9.2)
2	31.5 (t)	2.50 (dq, J = 3.8, 13.0); 1.90 (dq, J = 13.0, 3.8)	48.8 (d)	4.10 (tt, J = 13.0, 4.4)	31.5 (t)	2.15 (dddd, J = 13.4, 9.5, 9.2, 5.8); 2.05 (dddd, J = 13.4, 9.2, 7.4, 4.5)
3	42.8 (t)	1.28 (dt, J = 3.8, 13.0); 1.05 (dt, J = 13.0, 3.8)	42.5 (t)	1.80 (m, J = 4.4); 2.05 (m, J = 13.0)	32.5 (t)	2.35 (ddd, J = 14.0, 9.5, 4.5); 1.31 (ddd, J = 14.0, 7.4, 5.8)
4	71.2 (s)		41.0 (d)	1.35 (m, J = 6.6)	50.3 (s)	
5	47.7 (d)	0.44 (d, J = 4.0)	73.3 (s)		69.8 (d)	2.95 (d, J = 9.3)
6	23.0 (d)	0.53 (dd, J = 9.2, 4.0)	114.3 (d)	5.22 (br s)	30.7 (d)	0.30 (t, J = 9.3)
7	21.0 (d)	0.45 (m)	143.0 (s)		27.7 (d)	0.35 (dt, J = 9.3, 5.7)
8	16.8 (t)	1.73 (m, J = 13.9, 6.0); 1.43 (ddd, J = 13.9, 6.0, 4.0)	23.5 (t)	1.85 (m, J = 11.3); 1.60 (m, J = 11.3, 6.7)	14.7 (t)	1.48 (ddd, J = 13.8, 7.8, 5.7); 0.75 (ddd, J = 13.8, 6.6, 5.7)
9	39.5 (t)	1.82 (ddd, J = 12.1, 6.0, 4.0); 0.45 (dd, J = 12.1, 6.0)	30.5 (t)	0.90–0.85 (m, J = 6.7)	33.7 (t)	1.75 (dd, J = 14.6, 6.6); 1.23 (dd, J = 14.6, 7.8)
10	40.1 (s)		40.5 (s)		48.9 (s)	
11	16.2 (q)	1.30 (s)	22.3 (q)	0.70 (s)	22.5 (q)	0.95 (s)
12	30.1 (q)	0.85 (s)	15.5 (q)	0.80 (d, J = 6.6)	16.4 (q)	1.00 (s)
13	18.8 (s)		34.8 (d)	1.95 (m, J = 6.7)	19.0 (s)	
14	29.5 (q)	0.95 (s)	25.3 (q)	0.91 (d, J = 6.7)	28.5 (q)	0.88 (s)
15	16.7 (q)	0.75 (s)	21.8 (q)	0.91 (d, J = 6.7)	19.5 (q)	0.82 (s)

[a] Recorded in C_6D_6 at 300 MHz (^1H), 75 MHz (^{13}C). [b] Some coupling constants (^1H) not determined because of spectral overlap. J values are in hertz.

phytotoxicity with marine terpenoids.

The organic soluble extracts were partitioned,[3] and the observed biological activities were dispersed in the hexane and carbon tetrachloride solubles. The carbon tetrachloride fraction was permeated twice through Sephadex LH-20, first with methanol–dichloromethane (1:1) and then with methanol–acetonitrile (4:1) to give a mixture of sesquiterpenes. Resolution of what proved to be three constitutional isomers ($C_{15}H_{25}BrO$) was achieved by normal-phase HPLC on a bonded-phase (cyano) column, an approach employed previously in our work with diterpenes[4] and coumarins.[5] All three compounds were isolated as colorless oils.

Although proton-detected long-range heteronuclear multiple-quantum (HMBC) experiments are familiar because of their heteronucleus-detected analogues, the same cannot be said for any comparison of the ZQCOSY and COSY experiments. Since the ZQCOSY experiment has been utilized very heavily in the elucidation of the structures reported herein, some discussion of the optimization and interpretation of the data generated from this experiment is warranted.

The ZQCOSY pulse sequence proposed by Müller[6] is shown in Figure 1. In terms of implementation, the experiment has more in common with the still infrequently utilized proton double-quantum experiment than the now familiar COSY experiment. Zero-quantum coherence (ZQC) is excited during the preparation period, the fixed delays (τ) optimized as a function of $^1/_4(J_{HH})$. Dependence of the excitation on the duration of the fixed delay provides a degree of selectivity in the responses, which will be observed in the final spectrum. In our experience, the ZQCOSY experiment much more reliably identifies vicinal responses than does the COSY experiment.[7,8] After the evolution period (t_1), ZQC is reconverted to observable single-quantum coherence by the final 45° pulse.

Responses in the ZQCOSY experiment appear in the second- or zero-quantum frequency domain, F_1, at the algebraic difference of the chemical shifts of the correlated resonances relative to the transmitter frequency ($F_1 = F_2 = 0$ Hz). When a final read pulse

Uniform Excitation of Proton Zero Quantum Coherence

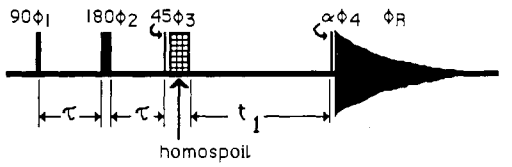

Figure 1. Uniform excitation of proton zero-quantum pulse sequence developed by Müller (Müller, L. *J. Magn. Reson.* **1984**, *59*, 326–331). Excitation is accomplished through the use of the 90°-τ-180°-τ-45° sequence. The homospoil pulse is optional and has anominal duration of 25–100 ms. Reconversion of zero to observable single-quantum coherence is accomplished by the α pulse. Generally, α = 45° to eliminate redundancies in the data matrix.

of 90° is employed, responses will be observed at the F_2 frequencies of the correlated resonances at $\pm F_1$. In this case, either F_1 response frequency may be employed to establish the correlation; the other redundant response at the opposite sign can be ignored. When a 45° read pulse is employed, which is the preferred method of performing the experiment, the F_2 responses located on the axis with a slope of −2 will be attenuated as a function of $(\tan \alpha/2)^2$ where α is the flip angle of the final pulse.[6] Coupled resonances, which are correlated by the ZQC, will thus be observed along a series of parallel diagonal axes defined by $F_2 = +2F_1$. Beneficially, halving the number of responses also provides quadrature detection in F_1, simultaneously reducing the possibility of degenerate overlap of responses without affecting the utility of the data.

The ZQCOSY spectrum of **1**, obtained with τ optimized for 5 Hz, is shown in Figure 2. (NMR data are given in Table I.) The five-spin system in ring A (part structure I) provides a

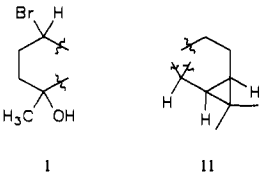

I II

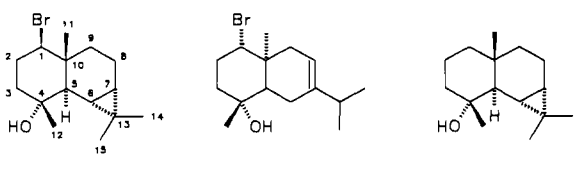

1 2 3

(3) Kupchan, S. M.; Britton, R. W.; Ziegler, M. F.; Sigel, C. W. *J. Org. Chem.* **1973**, *38*, 178.
(4) (a) Grode, S. H.; James, T. R., Jr.; Cardellina, J. H., II; Onan, K. D. *J. Org. Chem.* **1983**, *48*, 5203. (b) Hendrickson, R. L.; Cardellina, J. H., II *Tetrahedron* **1986**, *42*, 6565.
(5) Swager, T. M.; Cardellina, J. H., II *Phytochemistry* **1985**, *24*, 805.
(6) Müller, L. *J. Magn. Reson.* **1984**, *59*, 326.
(7) Zektzer, A. S.; Sims, L. D.; Castle, R. N.; Martin, G. E. *Magn. Reson. Chem.* **1988**, *26*, 287.
(8) Zektzer, A. S.; Martin, G. E.; Castle, R. N. *J. Heterocycl. Chem.* **1987**, *24*, 879.

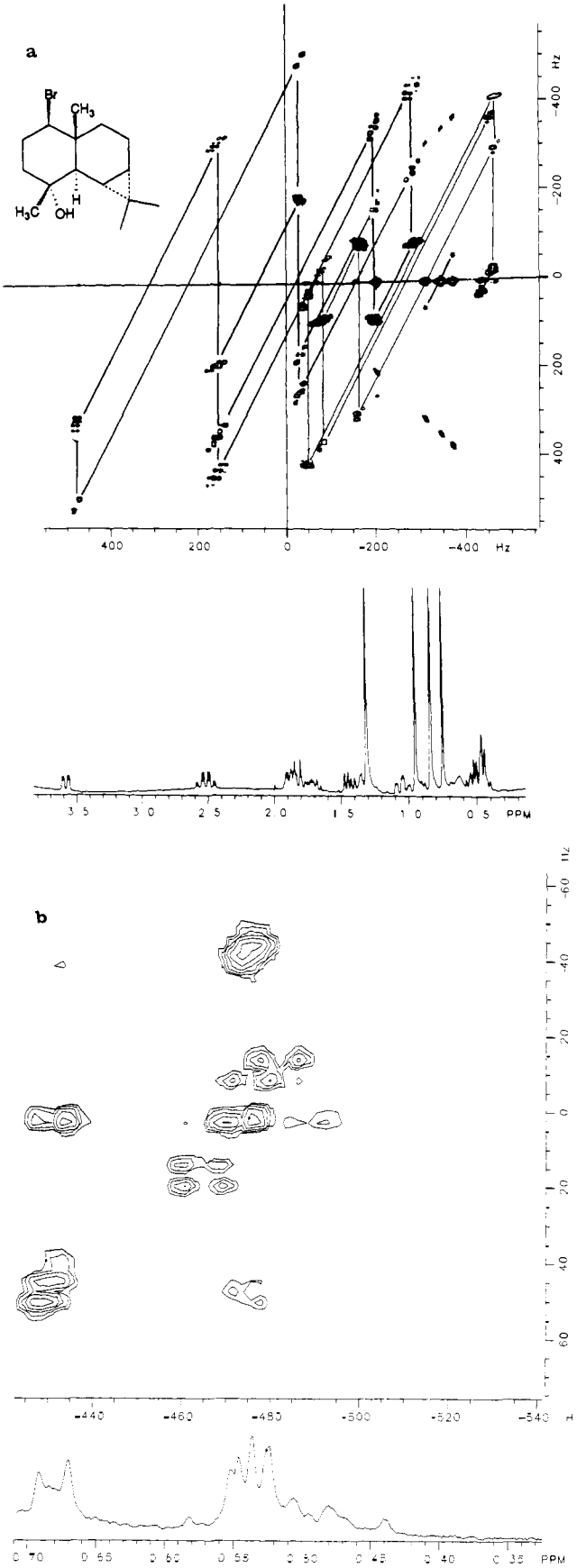

Figure 2. (a) 300-MHz ZQCOSY spectrum of **1** in C_6D_6. (b) Expansion of high-field region, 300-MHz ZQCOSY spectrum of **1**.

convenient system for initiating a discussion of the interpretation of the ZQCOSY spectrum. The bromomethine proton, H-1, resonating at δ 3.55 served as the starting point. Responses observed at the F_2 frequency of H-1 at 340 and 520 Hz in F_1

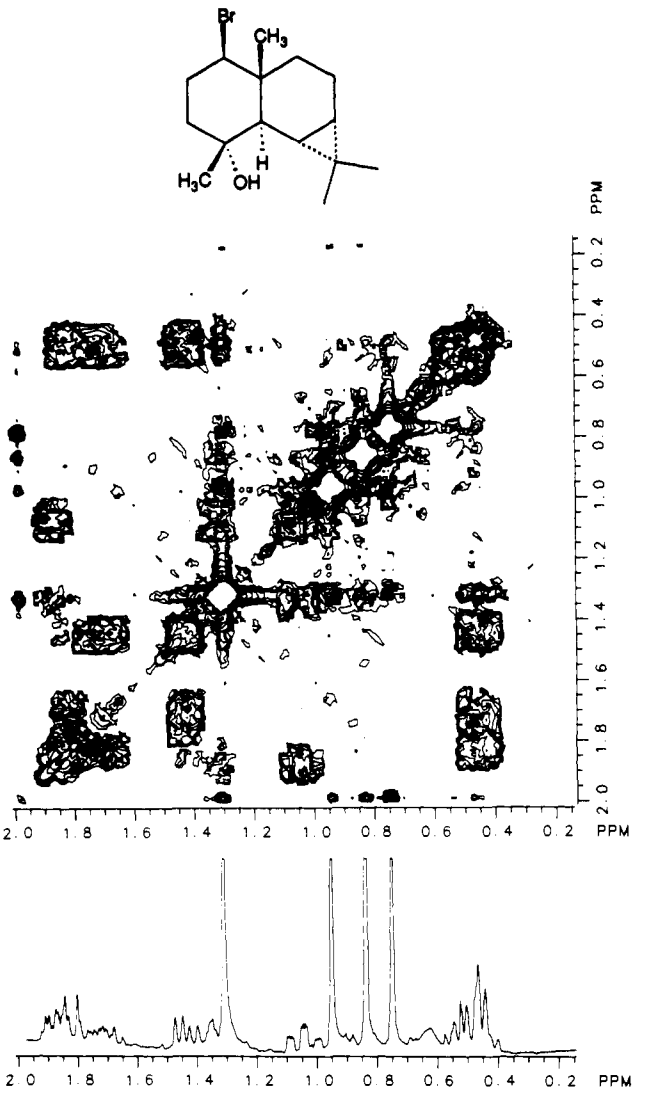

Figure 3. 300-MHz COSY spectrum of **1** in C_6D_6.

correlated the H-1 methine proton with its vicinal methylene neighbors resonating at δ 2.50 and 1.90 via responses observed in F_1 at −340 and −520 Hz, respectively. These observations suggested that the bromine was adjacent to a ring juncture as in **2**, isolated from the red alga *Laurencia sp.*[9] The geminal correlation for H-2a and H-2b was provided by the pair of responses observed at ±200 Hz in F_1 at the requisite F_2 frequencies of this pair. Continuing from H-2a (δ 2.50), correlations observed at ±370 and ±455 Hz in F_1 established the connectivity to H-3a and H-3b methylene protons resonating at δ 1.28 and 1.05, respectively, the former resonance being partially obscured by the 11-methyl resonance. H-2b was similarly correlated via responses observed at F_1 frequencies of ±175 and ±260 Hz. Finally, the geminal connectivity between H-3a and H-3b was established by the F_1 responses observed at ±80 Hz.

Disentangling the connectivity network for the seven proton resonances contained in ring B of **1** (part structure II) represented a more formidable challenge. Indeed, the four overlapped proton resonances between δ 0.40 and 0.60 were intractable in a conventional COSY spectrum (see Figure 3). Determining an unequivocal point of entry for the analysis of the spin system was a significant problem. However, once the H-9 methylene protons were located by means of a long-range correlation from the 11-methyl proton resonance in the HMBC spectrum (the 11-methyl resonance is long-range coupled to C-1, C-5, C-9, and C-10), the analysis could easily be undertaken. Thus, H-9a (δ 1.82) was

(9) Rose, A. F.; Sims, J. J. *Tetrahedron Lett.* **1977**, 2935.

correlated geminally to H-9b (δ 0.45) and vicinally to H-8a (δ 1.73). No correlation was observed between H-9a and H-8b (δ 1.43), although the latter did exhibit a geminal correlation to H-8a (±90 Hz). Both H-8a and H-8b were vicinally correlated to H-7 (δ 0.45), which was, in turn, correlated to H-6 (δ 0.53) and finally to H-5 (δ 0.44), the identity of which was confirmed by a long-range coupling in the HMBC experiment to the 12-methyl proton resonance. Finally, we should note that the geminal cyclopropyl methyls were also correlated to one another by a response in the ZQCOSY spectrum.

Proton long-range heteronuclear correlation (HMBC)[10] experiments permitted assembly of these part structures to give **1** as the correct structure. The methyl singlet at δ 1.3 was long-range correlated to the bromomethine (δ 67.5), a quaternary carbon at δ 40.1 and the methine at δ 47.7.

The relative stereochemistry illustrated for **1** was determined by means of difference NOE experiments. Enhancement of H-6 (8.2%) was observed upon irradiation of H-12. Irradiation of the H-11 methyl protons gave NOE's to H-8a (5.3%), H-2a (6.1%), and H-6 (9.7%). Irradiation of the bromomethine enhanced the signals for H-5/H-9a (9.7%). These data could be supported only by the configuration illustrated.

The absolute stereochemistry of **1** was determined by reductive elimination of the bromine with tri-*n*-butyltin hydride. The product obtained, **3**, was the enantiomer of natural (+)-maaliol, and, therefore, **1** possessed the 1*R*,4*R*,5*R*,6*S*,7*S*,10*R* stereochemistry and may be called 1(*R*)-bromo-*ent*-maaliol.

The second compound was also a tertiary alcohol, as indicated by an IR absorption at 3625 cm^{-1} and a ^{13}C NMR resonance at δ 73.3 (s). ^{13}C NMR signals at δ 143.0 (s) and 114.3 (d), together with the ^{1}H NMR signal at δ 5.22 (1 H, br s), indicated a trisubstituted olefin with only long-range coupling to the olefinic proton. Both COSY and ZQCOSY[6] experiments revealed coupling between the olefinic proton and nonequivalent methylene protons at δ 1.60 and 1.85, which were geminally coupled and also correlated to a second methylene group submerged by methyl signals from δ 0.9–0.85. A heptet at δ 1.95, coupled to overlapping methyl doublets centered at δ 0.91, comprised a vinyl isopropyl group and completed part structure III.

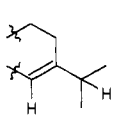

III

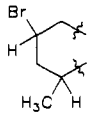

IV

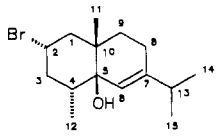

4

The ^{13}C NMR signal at δ 48.8 (d) and the ^{1}H NMR resonance at δ 4.10 (1 H, tt) were assigned to a bromine-bearing methine, the carbon upfield and the proton downfield of the corresponding resonances in **1**. The magnitude of the coincidentally equivalent coupling constants to the flanking methylene groups required the bromine to be equatorially situated and the axial hydrogen to have equivalent Karplus angles to its vicinal neighbors. The ZQCOSY spectrum located those neighboring methylenes at δ 1.80 and 2.25 (each a dd) and δ 1.80 and 2.05 (each a ddd). The former methylene had to reside next to a quaternary center, while the latter was coupled to a methine at δ 1.35, which, in turn, was coupled to a methyl group at δ 0.80. Thus, part structure IV was assembled.

Two sites of unsaturation, the tertiary alcohol, a quaternary methyl group (δ 0.70), and two fully substituted sp^3 carbons (δ 73.3 and 40.5) remained to be assigned. Long-range ^{1}H–^{13}C couplings were used to secure the structure of **4**. The methylene proton at δ 2.25 was correlated to the bromomethine (δ 48.8), the methyl-bearing quaternary carbon at δ 40.5 and the methylene carbon at δ 30.5. In turn, the methyl doublet at δ 0.80 was long-range coupled to the tertiary alcohol carbon (δ 73.3), the methine carbon at δ 41.0, and the methylene carbon at δ 42.5. The methyl group at δ 0.70 was correlated to methylenes at δ 47.8 and 30.5, along with the quaternary carbon at δ 73.3. Compound **4**, is, then, a eudesmane sesquiterpene with a unique placement of bromine and hydroxyl functionality.

The relevant data for the illustrated relative stereochemistry of **4** included enhancement of H-3 (6.2%) upon irradiation of H-6, H-2 (7.0%) upon irradiation of H-11, and H-3 (5.0 and 6.6%) and H-6 (7.5%) upon irradiation of H-12. A Drieding model representing the stereochemistry shown in **4** corroborated these data.

In the third sesquiterpene, neomeranol (**5**), the bromomethine carbon appeared at δ 59.0 (d), while the proton resonance was

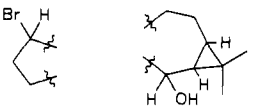

V VI

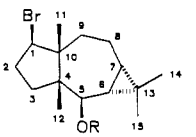

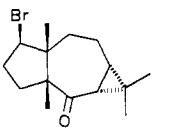

5 R= H 6

7 R=

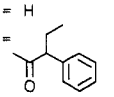

shifted downfield to δ 4.35 and appeared as a doublet of doublets. The ZQCOSY experiment[6] revealed that the bromomethine proton was vicinally coupled to geminal methylene protons at δ 2.15 and 2.05, which were in turn coupled to another methylene at δ 2.35 and 1.31. The latter methylene had no further couplings, and thus provided part structure V.

The IR absorption at 3620 cm^{-1} indicated a non-hydrogen-bonded hydroxyl group; and the proton resonance at δ 2.95 (1 H, d) and a ^{13}C NMR resonance at δ 69.8 (d) could be construed as representing a secondary alcohol, although the proton chemical shift appeared at an unusually high field. Neomeranol was oxidized in the presence of Jones' reagent to a ketone (**6**), shown by the loss of the proton resonance at δ 2.95 and the carbon signal at δ 69.8, concurrent with the appearance of a ^{13}C resonance at δ 211.0, thereby confirming the presence of a secondary alcohol in **5**.

The proton resonance at δ 2.95 was coupled to a cyclopropyl methine at δ 0.30 (1 H, dd), which, in turn, was coupled to another cyclopropyl methine at δ 0.35 (1 H, ddd). The ^{13}C NMR spectrum contained signals at δ 30.7 (d), 27.7 (d), and 19.0 (s) for the cyclopropane carbons. The ^{13}C NMR signals at δ 28.5 (q) and 19.5 (q) correlated with the methyl proton resonances at δ 0.88 (3 H, s) and 0.82 (3 H, s), respectively, indicating a geminal dimethyl array on the cyclopropane ring as in **1**. The methine at δ 0.35 was coupled to methylene protons at δ 1.48 (1 H, ddd) and 0.75 (1 H, ddd), which were coupled to another methylene at δ 1.75 (1 H, dd) and 1.23 (1 H, dd). Molecular models indicated a Karplus angle of approximately 90° between the protons at δ 0.75/1.75 and 1.48/1.23; there were no couplings observed in the NMR, and, thus, part structure VI was proposed.

Two sites of unsaturation, two quaternary methyl groups (δ 1.00 and 0.95), and two fully substituted sp^3 carbons (δ 50.3 and 48.9) remained to be assigned. Long-range ^{1}H–^{13}C couplings, determined by inverse-detected (proton) multiple-quantum techniques[10] (HMBC), were used to develop and confirm the structure of neomeranol (**5**). The methylene at δ 1.75 was correlated to both

(10) Bax, A.; Summers, M. F. *J. Am. Chem. Soc.* **1986**, *108*, 2093.

methyl-bearing quaternary carbons (δ 50.3 and 48.9) and the bromomethine at δ 59.0. In turn, the methyl at δ 0.95 was correlated to the bromomethine at δ 59.0, a methylene at δ 33.7, and both methyl-bearing quaternary carbons (δ 50.3 and 48.9). The methyl at δ 1.00 was long-range coupled to the secondary alcohol carbon at δ 69.8, a methylene at δ 32.5, and the methyl-bearing quaternary carbons (δ 50.3 and 48.9). The assignments of the two quaternary carbons were clarified by the long-range coupling of the methylene at δ 1.48 to the quaternary carbon at δ 48.9. The methyl at δ 0.82 was correlated to the quaternary cyclopropyl carbon at δ 19.0, two cyclopropyl methine carbons (δ 30.7 and 27.7), and the other methyl substituent on the cyclopropane, at δ 28.5, thus confirming the substitution of the cyclopropane ring. That the secondary alcohol methine at δ 2.95 was long-range coupled to the methyl group at δ 16.4, the cyclopropylmethine at δ 30.7, and the quaternary cyclopropyl carbon at δ 19.0 confirmed that the secondary alcohol was adjacent to the cyclopropyl group. In addition, the ketone **6** gave a UV absorption at 222 nm (ϵ = 540), consistent with Dauben's rules[11] for cyclopropyl conjugated ketones of this type.

The difference NOE study of **5** revealed the relative stereochemistry shown. The crucial data include enhancement of the hydroxylmethine H-5 (11.1%) upon irradiation of the bromomethine (H-1). The C-12 methyl group, when irradiated, gave enhancements at H-6 (12.1%) and H-3 (19.3%), and an NOE was also observed between H-11 and H-8 (10.1%). These data could only be accommodated by the relative stereochemistry shown in **5**, neomeranol. The relative stereochemistry having been secured, the absolute configuration was elucidated by Horeau's method.[12] The highly hindered secondary alcohol did not react with the anhydride of racemic 2-phenylbutyric acid but did succumb to treatment with the acid chloride,[13] producing **7** and leaving unreacted levorotatory acid with an optical yield of 21%. Therefore, the absolute configuration of neomeranol is 1*R*,4*R*,5*R*,6*R*,7*S*,10*R*.

The cytotoxic activity of **1**, **4**, and **5** was indicated by their toxicity to brine shrimp. The decalin ring system with the tertiary alcohol (**1** and **4**) was shown to have approximately twice the activity of the perhydroazulene ring system with a secondary alcohol. LD_{50} values were determined for **1**, **4**, and **5** to be 9, 8 and 16 μg/mL, respectively. All three novel sesquiterpenes were inactive ($LD_{50} > 20\mu g/mL$) in the KB in vitro assay; an investigation of minor metabolites from these active fractions is under way.

A cut-leaf assay was employed to test for phytotoxic activity.[14] Neomeranol displayed spot necrosis and chlorosis toward johnsongrass at 200 ppm after 72 h, while at 100 ppm only spot necrosis was detected. Neither **1** nor **4** showed any activity. The phytotoxicity profile is curiously the reverse of that for cytotoxicity.

The ketone **6** was found to have about the same brine shrimp toxicity as neomeranol (**5**) but no activity in the cut-leaf assay, thus establishing the importance of the secondary alcohol for phytotoxicity. An examination of the phytotoxicity of cyclopropyl-substituted alcohols might be warranted from these results.

The carbon skeleton of **5** has not been found previously among naturally occurring sesquiterpenes; we have, therefore, named the skeleton the neomerane system and **5** neomeranol. These major constituents of *N. annulata* are the first halogenated sesquiterpenes to be found in green algae.

Some time ago, Faulkner hypothesized that **1** might be the biosynthetic intermediate to both heterocladol and oppositol,[15] although it was unknown at the time. The biosynthesis of **1** and **5** could be rationalized as resulting from bromonium ion induced cyclizations of cyclodecadiene precursors. In the case of **5**, the initially formed carbocation would rearrange prior to nucleophilic addition of water. Alternatively the perhydroazulene skeleton could be formed directly; in either case, it would seem that the penultimate neopentyl carbocation is stabilized by the cyclopropane ring (see Scheme I). The carbon skeleton of **4** is that of eudesmane, but **4** is noteworthy for the novel positioning of the bromine and hydroxyl groups and is apparently not derived from a cyclodecadiene precursor.

Scheme I

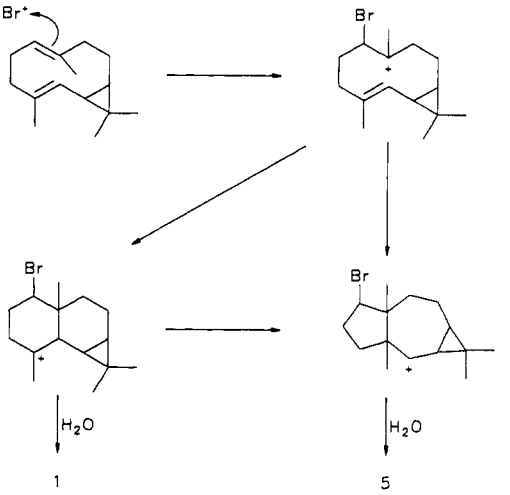

Experimental Section

General Procedures. All 1D NMR spectra were recorded on a Bruker WM-250 spectrometer; chemical shifts are reported in parts per million (δ, *J* = Hz) using $CDCl_3$ as solvent and internal standard. IR spectra were obtained with a NX Nicolet FT-IR spectrophotometer. Mass spectra were recorded on VG Industries MM16F and 7070 EHF mass spectrometers. Optical rotations were measured on a Perkin Elmer 241MC polarimeter.

All 2D NMR experiments were conducted on a Nicolet NT-300 wide-bore spectrometer operating at observation frequencies of 300.042 and 75.451 MHz for ^1H and ^{13}C, respectively. The spectrometer was controlled by a Model 293-C pulse programmer and equipped with a 5-mm $^1H/^{13}C$ dual tuned probe. Amplifier outputs were attenuated by 4 dB to prevent arcing in the probe, which gave pulse widths as follows: 90° ^1H pulse = 12.3 μs; 90° ^{13}C pulse = 18.3 μs. Proton pulses delivered from the decoupler were calibrated using the pulsed method of Bax[16] by which the 90° pulse = 32.8 μs.

To perform the proton-detected long-range heteronuclear multiple-quantum coherence experiments, the spectrometer was modified as described in our previous work.[7] The 90° ^{13}C pulse from the modified decoupler circuitry was calibrated using a solution of 99% ^{13}C-enriched [2-^{13}C]sodium acetate in deuterated water according to the method of Bax,[16] which gave a measured pulse length of 12.0 μs.

Homonuclear 2D NMR Experiments. Autocorrelated Proton (COSY) 2D NMR. All COSY 2D NMR spectra were acquired as 256 × 1K complex points. Data was acquired using the pulse sequence and 16-step phase cycle described by Bax et al.[17] A 1-s interpulse delay was uniformly employed. Data were processed using sinusoidal multiplication prior to both Fourier transformations with zero filling to 512 points prior to the second to afford a final data matrix consisting of 512 × 512 points with a digital resolution of 3.1 Hz/point in both frequency dimensions.

Proton Zero-Quantum Coherence 2D NMR 9(ZQCOSY). Zero-quantum coherence (ZQCOSY) 2D NMR experiments were performed using the pulse sequence devised by Müller[6] with an extended 64-step phase cycle as described in our previous work.[8,18] The data were acquired as 380 × 1K complex points with a 7-Hz optimization ($^1/_4(J_{HH})$ = 35.7 ms, unless otherwise indicated) of the τ delay in the excitation phase of the pulse sequence. The evolution time was set as a function of 0.75 × the F_2 dwell interval to accommodate connectivities between protons at the extremes of the chemical shift range. Spectral widths were ±805 and ±1100 Hz in F_2 and F_1, respectively. The sample was not spun

(11) Dauben, W. G.; Berezin, G. H. *J. Am. Chem. Soc.* **1967**, *89*, 3449.
(12) Horeau, A. In *Stereochemistry*; Kagan, H. B., Ed.; George Thieme: Stuttgart, 1977; Vol. 3, p 51.
(13) Cardellina, J. H., II; Barnekow, D. E. *J. Org. Chem.* **1988**, *53*, 882. For use of the acid halide of *O*-methyl mandelic acid, see: Trost, B. M.; Belletire, J. L.; Godleski, S.; McDougal, P. G.; Balkovec, J. M.; Baldwin, J. J.; Christy, M. E.; Ponticello, G. S.; Varga, S. L.; Springer, J. P. *J. Org. Chem.* **1986**, *51*, 2370.
(14) Sugawara, F.; Strobel, G. A.; Fisher, L. E.; VanDuyne, G. D.; Clardy, J. *Proc. Natl. Acad. Sci. U.S.A.* **1985**, *82*, 8291.
(15) Wratten, S. J.; Faulkner, D. J. *J. Org. Chem.* **1977**, *42*, 3343.
(16) Bax, A. *J. Magn. Reson.* **1983**, *52*, 76.
(17) Bax, A.; Freeman, R. *J. Magn. Reson.* **1981**, *44*, 542.
(18) Zektzer, A. S.; Martin, G. E. *J. Nat. Prod.* **1987**, *50*, 455.

to minimize t_1 noise, and four dummy scans were taken and discarded prior to the accumulation of data for each increment of t_1. Data were processed using sinusoidal multiplication prior to both Fourier transformations with zero filling to 512 points prior to the second to give a final data matrix comprised of 512 × 512 points. Digital resolution in the final spectra was 3.1 Hz/point in F_2 and 4.3 Hz/point in F_1.

Heteronuclear 2D NMR Experiments. Heteronuclear Chemical Shift Correlation via $^1J_{CH}$ with Selective Vicinal Proton Decoupling. Direct heteronuclear correlations were established using the pulse sequence described by Bax, which incorporates a BIRD pulse midway through the evolution period.[19] Data were acquired as 128 × 1K complex points with 32 acquisitions/block and a 1-s interpulse delay. Spectral widths were ±640 Hz in F_1 (^{1}H) and ±1780 Hz in F_2 (^{13}C). The τ delay in the BIRD pulse was optimized as a function of $^1/_2(^1J_{CH})$ = 3.57 ms for an assumed average coupling of 140 Hz. The fixed delays, Δ_1 and Δ_2, were set as a function of $^1/_2(^1J_{CH})$ and $^1/_3(^1J_{CH})$, respectively, which corresponds to 3.57 and 2.38 ms for an average one-bond coupling of 140 Hz. The data were processed using a 5-Hz exponential multiplication prior to the first Fourier transformation and a 2-Hz exponential multiplication and zero filling to 256 points prior to the second Fourier transformation to give a final data matrix consisting of 256 × 512 points with digital resolution of 5 Hz/point in F_1 and 7 Hz/point in F_2. Total acquisition time for the data was 1.5 h.

Long-Range Heteronuclear Chemical Shift Correlation with One-Bond Modulation Decoupling. Long-range heteronuclear chemical shift correlation was performed using the basic sequence of Freeman and Morris[20] modified by the inclusion of a BIRD pulse midway through the Δ_2 interval as described in our previous work.[21-23] Data were acquired as 96 × 2K complex points with 256 acquisitions taken per t_1 increment, and a 1-s interpulse delay was employed. Spectral widths were ±805 Hz in F_1 (^{1}H) and ±5210 Hz in F_2 (^{13}C). The τ interval in the BIRD pulse was optimized as above, giving a delay of 3.57 ms. The fixed defocusing delay, Δ_1, was optimized for 8 Hz, giving a duration of 62.5 ms (as a function of $^1/_2(^{LR}J_{CH})$); the duration of the refocusing delay, Δ_2 (where $\Delta_2 = {}^1/_3(^{LR}J_{CH}) = \Delta$-BIRD-$\Delta$ to give a net duration of $2\Delta + 2\tau$), was 41.6 ms (Δ = 17.23 ms, τ = 3.57 ms). The data were processed using a 10-Hz exponential multiplication prior to the first Fourier transformation and a 2-Hz exponential multiplication and zero filling prior to the second to afford a final data matrix consisting of 256 × 1K points. Final digital resolution was 6.3 Hz/point in F_1 and 10.2 Hz/point in F_2. Total accumulation time was 7.3 h.

Reverse-Detected (Proton) Long-Range Heteronuclear Chemical Shift Correlation via Heteronuclear Multiple-Quantum Coherence (HMBC). Proton-detected long-range heteronuclear chemical shift correlation via heteronuclear multiple-quantum coherence was performed using the pulse sequence described by Bax and Summers.[10] The low-pass J-filter portion of the experiment was optimized for an average one-bond heteronuclear coupling of 140 Hz (3.57 ms). The long-range delay, Δ, utilized to excite the heteronuclear multiple-quantum coherence was optimized for 60 ms (the sum of $\tau + \Delta$ = 63.6 ms, corresponding to a 7.9-Hz optimization). Proton T_1 relaxation times were measured to set the interpulse delay prior to beginning the experiment using the inversion–recovery pulse sequence. On this basis, the interpulse delay was set to 1.3 s. The sample was not spun to reduce t_1 noise, and four dummy scans were taken and discarded prior to commencing accumulation of the data for each t_1 increment. Data were acquired as 380 × 1K complex points with 96 acquisitions/block giving a total accumulation time of 13.2 h (overkill). Spectral widths were ±1780 Hz in F_1 (^{13}C) and ±1805 Hz in F_2 (^{1}H). The data was processed using a sinusoidal multiplication followed by 1.5-Hz exponential multiplication prior to the first Fourier transformation and zero filling to 512 points prior to the second Fourier transformation with double-exponential apodization. Final digital resolution was 3.1 Hz/point in F_2 and 7 Hz/point in F_1.

Collection, Extraction, and Separation. *N. annulata* was collected from several shallow water (−1 m) locations in Bermuda and stored at −5 °C in acetone prior to extraction. The acetone was filtered and reduced, in vacuo. The alga was then homogenized in a Waring blender with methanol, and the solvent was removed, in vacuo. The marc was then extracted with CH_2Cl_2 (twice, 24 h each). The aqueous suspension remaining after evaporation of the acetone and methanol extracts was equilibrated with the CH_2Cl_2 extracts; the organic phase was concentrated to a dark green oil. The 1984 collection yielded 225 mg of extract (from 19.4-g dry weight), and the 1986 collection yielded 3.02 g (from 435.6-g dry weight).

The 1984 extract was chromatographed on Sephadex LH-20 with MeOH–CH_2Cl_2 (1:1). Seven fractions were collected. Fraction 6 (46 mg) was then chromatographed on Sephadex LH-20 with MeOH–CH_3CN (4:1) to give five fractions. Fraction 2 (23.9 mg) was then submitted to HPLC on a Beckman Altex Ultrasphere cyano column (1 × 25 cm) with hexane–CH_2Cl_2 (4:1) to give **1** (19 mg) and **4** (15 mg).

The Kupchan style partition scheme[3] was used to separate the 1986 extract, yielding hexane (1.79 g), CCl_4 (750 mg), $CHCl_3$ (223 mg), and H_2O (107 mg) solubles.

The CCl_4 solubles were chromatographed on Sephadex LH-20 with MeOH–CH_2Cl_2 (1:1) to give 10 fractions. Fraction 6 (246 mg) was dissolved in MeOH–CH_3CN (4:1) and filtered; the filtrate was chromatographed on Sephadex LH-20 with MeOH–CH_3CN (4:1) to yield seven fractions. Fraction 5 (163 mg) was then submitted to HPLC on a Beckman Altex Ultrasphere-Cyano column (1 × 25 cm) with hexane–CH_2Cl_2 (4:1), yielding **1** (92 mg), **4** (26 mg), and **5** (29 mg).

The hexane solubles were chromatographed on Bio-Beads S-X4 with hexane–CH_2Cl_2–EtOAc (4:3:1), yielding 13 fractions. Fraction 7 (621 mg) was then chromatographed by the same sequence as the CCl_4 solubles, yielding **1** (195 mg), **4** (177 mg), and **5** (54 mg).

1(*R*)-Bromo-*ent*-maaliol (1*H*-cyclopropa[*a*]naphthalen-7-ol, decahydro-1,1,3a,7-tetramethyl, [1a*S*-(1aα,3aβ,4β,7β,7aα,7bβ)]) (1): colorless oil, $[\alpha]_D$ −45.6° (*c* 1.62, $CHCl_3$); high-resolution EIMS *m/z* 300.1083 (M^+, 10%, $C_{15}H_{25}BrO$ requires 300.1105), 282 (10), 267 (4), 220 (15), 202 (35), 109 (18), 43 (100); ν_{max} CCl_4 3665, 2935, 1375, 1175 cm^{-1}; 0.06% dry weight.

8a-Naphthalenol, 3-bromo-1,2,3,4,4a,5,6,8a-octahydro-1,4a-dimethyl-7-(1-methylethyl), (1α,3α,4aβ,8aβ) (4): colorless oil, $[\alpha]_D$ −5.9° (*c* 1.70, $CHCl_3$); high-resolution EIMS *m/z* 300.1083 (M^+, 2%, $C_{15}H_{25}BrO$ requires 300.1105), 282 (10), 267 (4), 220 (20), 202 (10), 152 (100), 109 (77); ν_{max} CCl_4 3625, 2930, 1160 cm^{-1}; 0.04% dry weight.

Neomeranol (1*H*-cyclopropa[*e*]azulen-7-ol, decahydro-1,1,3a,6a-tetramethyl, [1a*S*-(1aα,3aβ,4β,6aβ,7β,7aα)]) (5): colorless oil, $[\alpha]_D$ −27.3° (*c* 1.65, $CHCl_3$); high-resolution EIMS *m/z* 300.1077 (M^+, 4%, $C_{15}H_{25}BrO$ requires 300.1105), 203 (18), 109 (38), 85 (100); ν_{max} CCl_4 3625, 2945, 1250 cm^{-1}; 0.02% dry weight.

Oxidation of Neomeranol. To a solution of 15 mg (0.05 mmol) of **5** in 1 mL of acetone was added 300 μL of Jones' reagent; the mixture was warmed to 40 °C and stirred for 5 min. The reaction was then quenched by adding 2-propanol until the red-orange color disappeared; the mixture was reduced, in vacuo, and extracted with $CHCl_3$ (3 × 10 mL). The $CHCl_3$ phase was then evaporated to yield 14.6 mg (98%) of neomeranone (**6**), a colorless oil: $[\alpha]_D$ −34.5° (*c* 0.87, $CHCl_3$); EIMS *m/z* 298 (M^+, 8%, $C_{15}H_{23}BrO$), 219 (25), 123 (50), 95 (100); λ_{max} EtOH 222 nm (ϵ = 540); ν_{max} CCl_4 2980, 2950, 1690, 1380 cm^{-1}; ^{1}H NMR (C_6D_6) δ 4.15 (1 H, dd), 2.48 (1 H, dddd), 2.20 (1 H, dddd), 1.93 (1 H, ddd), 1.89 (1 H, dd), 1.79 (1 H, dd), 1.48 (1 H, ddd), 1.25 (1 H, d), 1.20 (3 H, s), 1.10 (1 H, ddd), 0.90 (3 H, s), 0.83 (3 H, s), 0.80 (3 H, s), 0.75 (1 H, ddd), 0.45 (1 H, ddd); ^{13}C NMR ($CDCl_3$) δ 211.0 (s), 59.4 (s), 56.2 (d), 48.3 (s), 34.1 (t), 33.2 (t), 32.2 (d), 31.6 (q), 28.3 (d), 23.6 (s), 21.0 (q), 20.1 (q), 16.8 (q).

Debromination of 1(*R*)-Bromo-*ent*-maaliol. 1(*R*)-Bromo-*ent*-maaliol (21.9 mg, 0.072 mmol) was dissolved in 1 mL of benzene-d_6; to this was added tri-*n*-butyltin hydride (23.2 mg, 0.080 mmol) and a catalytic amount of 2,2′-azobis(2-methylpropionitrile).[24] The mixture was irradiated by a sunlamp for $^1/_2$ h, at which time the ^{1}H NMR showed complete conversion of starting material. The mixture was then reduced in vacuo, and the residue was dissolved in dimethylformamide (DMF) and treated with saturated aqueous KF. The precipitated tri-*n*-butyltin fluoride was removed by filtration through Celite.[25] The filtrate was partitioned between diethyl ether (200 mL) and water (4 × 20 mL). The ether layer was separated and dried ($NaSO_4$). Evaporation of solvent, in vacuo, yielded 16.7 mg of (−)-maaliol (**3**): $[\alpha]_D$ −37.8° (*c* 1.48, $CHCl_3$) and −20.3° (*c* 1.48, EtOH) [lit.[26] for (+)-maaliol $[\alpha]_D$ +38.7° (*c* 4.0, $CHCl_3$) and +21.7° (*c* 5.0, EtOH)]; ^{1}H NMR (C_6D_6) δ 1.98–1.78 (2 H, m), 1.59–1.45 (2 H, m), 1.40–1.33 (3 H, m), 1.23–1.13 (1 H, m), 1.16 (3 H, s), 1.07–1.00 (1 H, m), 1.01 (6 H, s), 0.92–0.72 (1 H, m), 0.83 (3 H, s), 0.66–0.40 (4 H, m); ^{13}C NMR ($CDCl_3$) δ 71.9 (s), 46.8 (d), 41.0 (t), 40.9 (t), 39.8 (t), 32.3 (s), 29.6 (q), 28.5 (q), 21.0 (d), 19.3

(19) Bax, A. *J. Magn. Reson.* **1983**, *53*, 517.
(20) Freeman, R.; Morris, G. A. *J. Chem. Soc., Chem. Commun.* **1978**, 684.
(21) Quast, M. J.; Zektzer, A. S.; Martin, G. E.; Castle, R. N. *J. Magn. Reson.* **1987**, *71*, 554.
(22) Zektzer, A. S.; John, B. K.; Castle, R. N.; Martin, G. E. *J. Magn. Reson.* **1987**, *72*, 556.
(23) Zektzer, A. S.; John, B. K.; Martin, G. E. *Magn. Reson. Chem.* **1987**, *25*, 752.
(24) vander Kerk, G. J. M.; Noltes, J. G.; Luitjen, J. G. A. *J. Appl. Chem.* **1957**, *7*, 366.
(25) Leibner, J. E.; Jacobs, J. *J. Org. Chem.* **1979**, *44*, 449.
(26) Narayanan, C. S.; Kulkarni, K. S.; Vaidya, A. S.; Kanthamani, S.; Lakshmi Kumari, G.; Bapat, B. V.; Pakanikar, K. S.; Kulkarni, S. N.; Kelkar, G. R.; Bhattacharyya, S. C. *Tetrahedron* **1964**, *20*, 963.

(d), 18.8 (t), 18.0 (t), 17.4 (s), 15.7 (q), 15.6 (q); MS (relative intensity) m/z 222 (M^+, 24), 204 (100), 189 (99), 161 (50), 137 (54), 109 (83), 43 (74).

Preparation of the 2-Phenylbutanoyl Ester of Neomeranol. The 2-phenylbutyrate of neomeranol (**5**) was prepared from 8.4 mg of neomeranol and the acid chloride using procedures described recently.[13] The crude product was purified by HPLC (Ultrasphere-Cyano, 4:1 hexane-CH_2Cl_2) to give **7**, 3.8 mg: $[\alpha]_D$ -10.5° (c 0.38, $CHCl_3$); ^1H NMR ($CDCl_3$) δ 7.3-7.2 (5 H, br s), 4.64 (1 H, dd), 4.45 (1 H, dd), 3.45 (1 H, m), 2.28-2.20 (2 H, m), 1.91-1.50 (4 H, m), 1.35-1.10 (3 H, m), 1.08 (3 H, s), 0.98-0.95 (2 H, m), 0.91 (3 H, s), 0.89 (3 H, t), 0.78 (3 H, s), 0.70 (3 H, s), 0.56 (1 H, dd); MS (relative intensity) m/z 448 (M^+, 0.5), 367 (52), 282 (16), 203 (66), 119 (100), 95 (63). The optical rotation of the acid recovered from unreacted acid chloride was $[\alpha]_D$ -15.6° (c 0.45, $CHCl_3$), corresponding to an optical yield of 21%.[12]

Acknowledgment. We thank L. J. Sears for the accurate mass measurements and Professor T. Livinghouse for helpful suggestions. This work was supported by the Office of Sea Grant, Department of Commerce, the Montana Agricultural Experiment Station, and, in part, by Grant CA 35905 from the National Cancer Institute and Grant E-792 from the Robert A. Welch Foundation.

Revisiting Kaolinite Dehydroxylation: A ^{29}Si and ^{27}Al MAS NMR Study

J. F. Lambert, W. S. Millman, and J. J. Fripiat*

Contribution from the Laboratory for Surface Studies and Department of Chemistry, University of Wisconsin—Milwaukee, Milwaukee, Wisconsin 53201. *Received June 20, 1988*

Abstract: The ^{29}Si and ^{27}Al MAS NMR spectra of kaolinite are easily interpreted in terms of a Q^3 environment for silicon and of an octahedral configuration of aluminum. Upon progressive dehydroxylation, these spectra become more complex. For a degree of dehydroxylation (α) between 1/10 and 9/10, three ^{27}Al resonances are observed at +3, +28, and +55 ppm. The octahedral component decreases in intensity as α increases, whereas the other two become dominant. The line at +28 ppm is assigned to pentacoordinated Al, as suggested by Gilson et al. (*J. Chem. Soc., Chem. Commun.* **1987**, 91). The +55-ppm line is attributed to tetrahedrally coordinated Al. Simultaneously, the -91-ppm (initial) component of the ^{29}Si spectrum decreases in intensity, while at least two components corresponding to more shielded Si nuclei grow in intensity. As α increases beyond 9/10, further shifts are observed in the ^{29}Si spectra as mentioned by Meinhold et al. (*J. Mater. Sci. Lett.* **1985**, *4*, 163). Ultimately a line at -109 ppm suggests a significant proportion of the ^{29}Si nuclei being in a Q^4 environment, while the ^{27}Al spectrum is reminiscent of that of a spinel-like material. The relationships between the ^{29}Si and ^{27}Al spectra are discussed and compared with IR data in the 1200-400-cm^{-1} range and with earlier results on ^1H (static) NMR.

The mechanism by which kaolinite loses water has attracted much attention over the past century. The structure of the material has been well characterized, and numerous studies have been devoted to the kinetic process. The structural arrangement in the dehydration product, i.e., metakaolinite, was studied by several groups, the most classical work being that of Brindley and Nakahira.[1] They concluded that during the dehydration the original atomic ordering along the a and b axes was maintained, but that it disappeared along the c axis.[2] Accordingly, they showed that the coordination number of the aluminum changes from 6-fold to 4-fold and that the reaction proceeds by successive dehydroxylation of the octahedral layers. Indeed, the intensity of the [001] X-ray reflection shows an inverse linear decrease with the extent of dehydroxylation (α). Moreover, up to $\alpha = 0.6$, the second moment of the ^1H NMR resonance line is nearly constant.[3] If the dehydroxylation occurred by the growth of randomly distributed nuclei, the average proton-proton distance should increase with α and the second moment should decrease rapidly as predicted by its $1/r^6$ dependence. This behavior of the second moment was recently confirmed,[4] in a study of the proton resonance as a function of α, covering a range of $\alpha \approx 0$ to $\alpha = 0.97$. For $\alpha < 0.7$ the second moment was invariant. However, for $0.7 < \alpha \leq 0.97$, the remaining protons distribute themselves among two population of sites. This latter conclusion was reached by distinguishing between the proton-proton interaction and the proton-aluminum interaction using the Carr-Purcell pulse sequence to separate the heteronuclear dipolar coupling (plus shielding anisotropy) from the homonuclear dipolar broadening. In the range $\alpha > 0.7$, the proton-proton second moment decreases from 6 to 1 G^2, whereas the ^1H-^{27}Al second moment remains at about 1.4 G^2. The proton population with the decreasing ^1H-^1H moment was assumed to be within shrinking patches of Al(OH) octahedra. The second population was suggested to be composed of isolated protons interacting with aluminum.

Meinhold et al.[5] were among the first to study the high-temperature transformation of metakaolinite into mullite, which occurs above 900 °C, using high-resolution solid-state ^{27}Al and ^{29}Si NMR. In spite of relatively poor resolution (the field was 4.7 T and the spinning rate was 2.6 kHz), they observed a ^{27}Al resonance at 35 ppm in addition to those at 65 and 0 ppm for tetrahedrally and octahedrally coordinated aluminum, respectively. The resonance at 35 ppm was upfield of any previously reported resonance for tetrahedrally coordinated aluminosilicates. In conjunction with the transformations of the ^{27}Al spectra, the ^{29}Si spectra broadened and shifted from that observed in kaolinite (-91.5 ppm) to about -100 ppm. At temperatures above 900 °C, the ^{29}Si spectrum was found to consist of a resonance at about -110 ppm with a shoulder at about -88 ppm. The upfield shift was considered to reflect a decrease in the number of Al groups bonded to the SiO_4 tetrahedral units.

In studying metakaolinite at higher fields and spinning rates (9.4 T), Gilson et al.[6] went further in interpreting the ^{27}Al MAS

* To whom all correspondence should be addressed.

(1) Brindley, G. W.; Nakahira, M. *Mineral. Mag.* **1958**, *31*, 781.
(2) Brindley, G. W.; Nakahira, M. *J. Am. Ceram. Soc.* **1959**, *42*, 311.
(3) Gastuche, M. C.; Toussaint, F.; Touilleaux; Fripiat, J. J.; Van Meersch, M. *Clay Mineral. Bull.* **1963**, *5*, 227.
(4) Otero-Arean, C.; Letellier, M.; Gerstein, B. C.; Fripiat, J. J., *Proceedings of the International Clay Conference, 1981*; (Van Olphen and Veniale, Eds.; Elsevier, New York, 1982; p 73.
(5) Meinhold, R. H.; MacKenzie, K. J. D.; Brown, I. W. M. *J. Mater. Sci. Lett.* **1985**, *4*, 163.

0002-7863/89/1511-3517$01.50/0